Received: 1 July 2023 | Accepted: 22 August 2023

DOI: 10.1002/pamm.202300232

RESEARCH ARTICLE

Simulation of vibrating droplets using a phase field approach

Jana Kunz[1] | **Xenia Rutz**[1] | **Simon Stephan**[2] | **Hans Hasse**[2] | **Ralf Müller**[3]

[1]Institute of Applied Mechanics, University of Kaiserslautern-Landau (RPTU), Kaiserslautern, Germany

[2]Laboratory of Engineering Thermodynamics, University of Kaiserslautern-Landau (RPTU), Kaiserslautern, Germany

[3]Institute for Mechanics, Technical University of Darmstadt, Darmstadt, Germany

Correspondence
Jana Kunz, Institute of Applied Mechanics, University of Kaiserslautern-Landau (RPTU), 67663 Kaiserslautern, Germany.
Email: jana.kunz@mv.rptu.de

[Correction added on 08 September 2023, after first online publication: Projekt DEAL funding statement has been added.]

Funding information
Deutsche Forschungsgemeinschaft, Grant/Award Numbers: 172116086, SFB 926

Abstract

Droplet vibration is an important phenomenon in many technical applications. Correctly predicting the occurring behaviour such as droplet detachment is a challenge for numerical simulations. In this work, a so-called Navier-Stokes-Korteweg model that couples a gas-liquid phase field to the Navier-Stokes equations is used to simulate a droplet on a horizontally vibrating surface. Additionally, the equilibrium state of a static droplet on a fixed wall is simulated and the eigenshapes of the static system are investigated. It is found that this static eigenvalue analysis yields possible modes of the dynamic system, and some of the obtained eigenshapes can be recovered in the dynamic simulation.

KEYWORDS
droplet vibration, phase field, wetting

1 | INTRODUCTION

The wetting behaviour of vibrating droplets plays an important role in technical applications such as the cooling of electronic devices [1–3]. Due to the high underlying non-linearity, the behaviour of vibrating droplets is still not fully understood. Especially for the case of small micro-droplets, experimental investigations are difficult to perform and it is therefore challenging to investigate the influence of all relevant parameters such as viscosity, density, surface tensions, and so forth. Hence, numerical simulations are a crucial tool in order to improve the understanding of the phenomenon of droplet vibration.

In this work, the phase field model developed by Diewald et al. [2, 4] is used where an order parameter distinguishes between the gas and the liquid phase. Both the static model from [4] and the extended dynamic model from [2] are employed here.

2 | BASIC CONCEPTS OF THE PHASE FIELD MODEL

In this work, the phase field model from [4] is used to describe the continuous transition between gas and liquid. It is characterised by the phase field parameter φ that can be understood as a dimensionless density

$$\varphi = \frac{\rho - \rho_\mathrm{g}}{\rho_\mathrm{l} - \rho_\mathrm{g}},$$

where ρ is the density and ρ_g, ρ_l are the bulk densities of the gas and liquid phase, respectively. With this definition, $\varphi = 0$ describes the gas and $\varphi = 1$ the liquid phase.

The free energy density f is described as

$$f(\varphi, \nabla\varphi) = f_1(\varphi) + f_2(\nabla\varphi) = 12\frac{\gamma_\mathrm{lg}}{l^e}\varphi^2(1-\varphi)^2 + \frac{3}{4}\gamma_\mathrm{lg} l^e |\nabla\varphi|^2 \tag{1}$$

and is composed of a local term $f_1(\varphi)$ and a non-local term $f_2(\nabla\varphi)$. In earlier works of our group, we have also used a model from molecular thermodynamics in this phase field approach [2, 5–7]. For the present concept model study, the more simple double-well potential is used as $f_1(\varphi)$. In Equation (1), γ_lg is the surface tension between liquid and gas and l^e is the width of the interface.

3 | STATIC MODEL

To calculate the equilibrium state for a given initial density distribution, a static model that neglects dynamic effects can be used. For this purpose, a free energy functional F can be computed from the free energy density in Equation (1):

$$F = \int_\Omega f(\varphi, \nabla\varphi)\mathrm{d}V + \lambda \int_\Omega [\varphi - \varphi_0]\mathrm{d}V + \int_{\partial\Omega_S} \phi(\varphi)\mathrm{d}S, \tag{2}$$

where Ω is the calculation domain and $\partial\Omega_S$ the part of its boundary that is defined by a solid wall. In addition to the contribution from the free energy density of the domain, a constraint with the Lagrange multiplier λ is added in Equation (2) to ensure mass conservation in the domain, given by the initial distribution φ_0. Furthermore, a surface energy contribution $\phi(\varphi)$ is added. It is an integral over the surface tension on the solid boundary of the domain:

$$\phi(\varphi) = h(\varphi)\gamma_\mathrm{sl} + (1 - h(\varphi))\gamma_\mathrm{sg}, \quad \text{with} \quad h(\varphi) = \varphi^3\left(6\varphi^2 - 15\varphi + 10\right), \tag{3}$$

where the interpolation function $h(\varphi)$ from [8] is used to interpolate between the surface tensions of the solid-liquid and solid-gas interfaces γ_sl and γ_sg.

In order to find the equilibrium solution, the free energy functional F from Equation (2) is minimised and the equation

$$\delta F = 0 \quad \Rightarrow \quad \frac{\partial f}{\partial \varphi} - \mathrm{div}\frac{\partial f}{\partial \nabla\varphi} = 0 \tag{4}$$

is solved with the finite element method. As this proves numerically challenging depending on the initialisation, an evolution equation of Allen-Cahn type is used to approach this solution state:

$$\frac{\partial \varphi}{\partial t^*} = -M\left[\frac{\partial f}{\partial \varphi} - \mathrm{div}\frac{\partial f}{\partial \nabla\varphi}\right], \tag{5}$$

where M is a mobility constant. As dynamic effects were neglected in the derivation of this model, t^* in Equation (5) is a pseudo time used to relax into the static solution rather than a physical time. When the solution field has evolved sufficiently close to the static solution, Equation (4) can then be solved directly.

4 | DYNAMIC MODEL

The dynamic behaviour of the fluid system can be described by the Navier-Stokes equations:

$$\dot{\varphi} + \varphi \mathrm{div}\vec{v} = 0 \tag{6}$$

$$\varphi\dot{\vec{v}} = \mathrm{div}\boldsymbol{\sigma}\,, \tag{7}$$

where $\vec{v}$ is the velocity vector and $\boldsymbol{\sigma}$ is the stress tensor. Body forces and gravity are neglected in Equation (7). In comparison to standard Navier-Stokes equations, Equation (6) and (7) are written in terms of the phase field parameter φ that takes on the role of the density.

The stress tensor $\boldsymbol{\sigma}$ in Equation (7) is used to couple the Navier-Stokes equations to the phase field as described in [2]. To achieve this, the stress tensor is decomposed as follows:

$$\boldsymbol{\sigma} = \boldsymbol{\sigma}^{\mathbf{v}} + \boldsymbol{\sigma}^{\psi} \tag{8}$$

$$\boldsymbol{\sigma}^{\mathbf{v}} = 2\eta(\varphi)\left(\nabla^s\vec{v} - \frac{1}{3}tr\left(\nabla^s\vec{v}\right)\mathbf{1}\right) \tag{9}$$

$$\boldsymbol{\sigma}^{\psi} = (f - \varphi\mu)\mathbf{1} - \left(\frac{\partial f}{\partial\nabla\varphi} \otimes \nabla\varphi\right) \tag{10}$$

$$\mu = \frac{\partial f}{\partial\varphi} - \mathrm{div}\frac{\partial f}{\partial\nabla\varphi}\,, \tag{11}$$

where $\boldsymbol{\sigma}^{\mathbf{v}}$ is the viscous stress tensor that accounts for the stress in the bulk phases, and $\boldsymbol{\sigma}^{\psi}$ is the so-called Korteweg stress tensor which incorporates the stress in the gas-liquid interface. In Equation (10), the chemical potential μ is introduced as an additional variable. It can be expressed in terms of the free energy density as written in Equation (11). The viscosity η is modeled as a simple exponential function of the order parameter:

$$\eta(\varphi) = \exp(a\varphi) + b\,, \tag{12}$$

with a and b as material constants. The approach from Equations (10)–(11) was first introduced by Korteweg in 1901 [9] and presents an efficient way to formulate the dynamic model for the gas-liquid phase field as it comes without an additional diffusion equation. As shown in [10], the static model described by Equations (2)–(4) can be derived from the dynamic model as a special case where $\vec{v} = \vec{0}$. The chemical potential μ then plays the role of the Lagrange multiplier with $\mu = -\lambda$. To incorporate the surface tension contributions from the solid-fluid boundary, the surface energy function from Equation (3) is included in the model via a Neumann boundary condition:

$$\frac{\partial f}{\partial\nabla\varphi} \cdot \vec{n} + \frac{\partial\phi}{\partial\varphi} = 0\,, \tag{13}$$

with ϕ from Equation (3).

5 | EIGENVALUE ANALYSIS

As a numerical example, the static equilibrium solution of a two dimensional droplet on a planar solid wall is calculated. The surface tensions were chosen as $\gamma_{\mathrm{lg}} = 0.581$ and $\gamma_{\mathrm{sl}} = \gamma_{\mathrm{sg}} = 0.1$, which yields a resulting static equilibrium contact angle of 90°.

The eigenshapes of the resulting droplet are then investigated. For this purpose, an eigenvalue analysis of the system matrix of the finite element system is conducted. The same procedure was used by Diewald et al. in order to analyse the

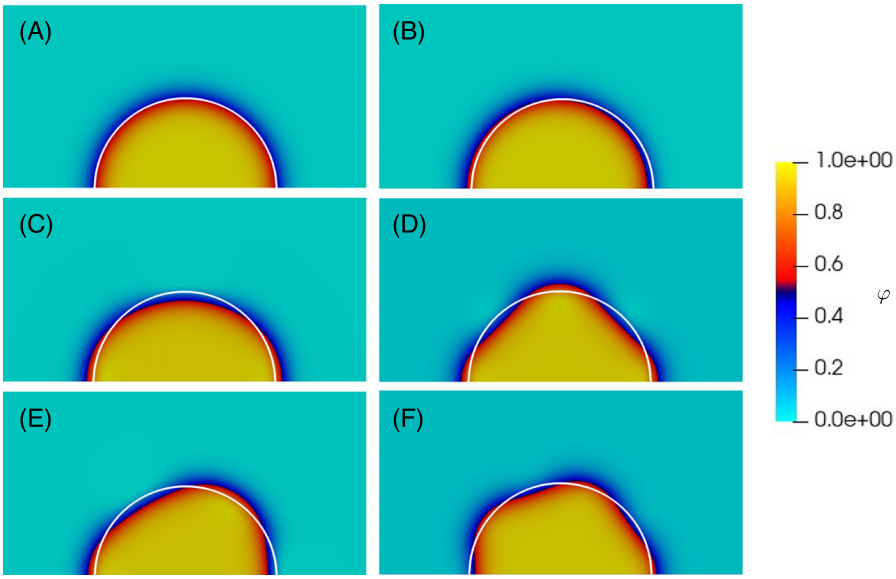

FIGURE 1 (A) Static solution of a droplet on a flat surface with a contact angle of 90°. (B)–(F) Eigenshapes $\varphi + ku_i$ of the first five eigenvalues. The white contour indicates $\varphi = 0.5$ in the solution state.

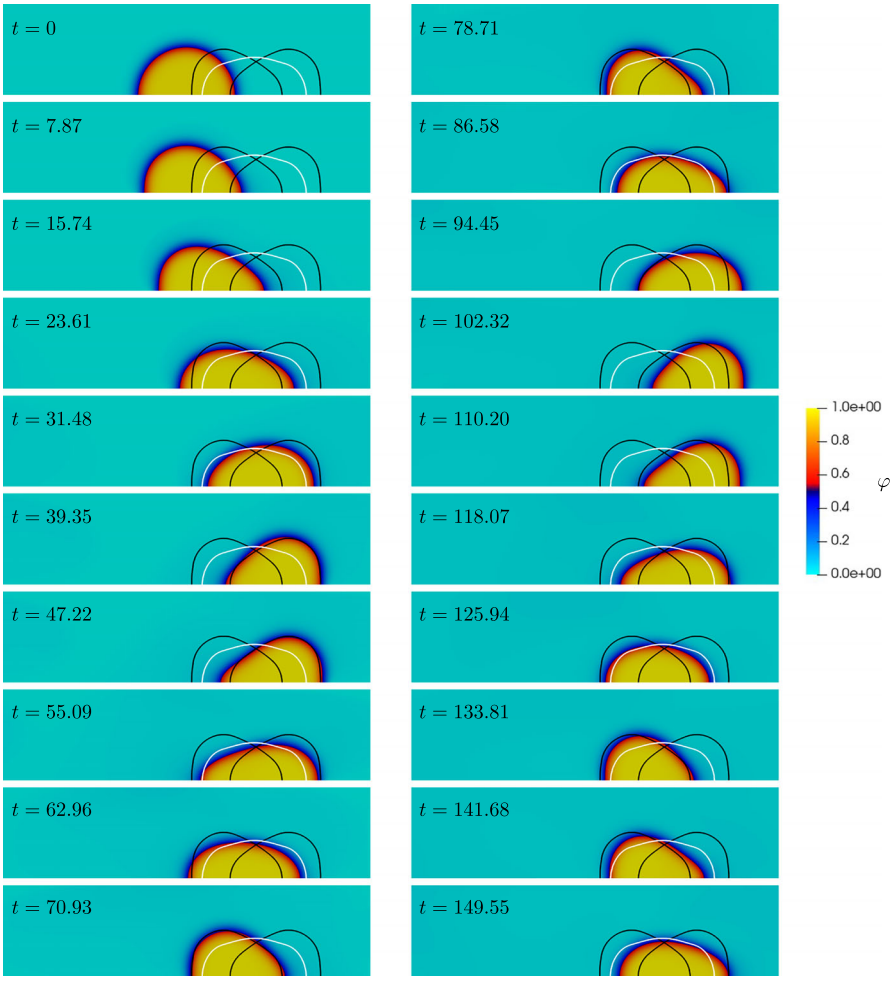

FIGURE 2 Snapshots of the simulation of a droplet with a static contact angle of 90° on a vibrating wall with $A = 10$ and $\omega = 0.1$. The black and white contours show eigenshapes of the static solution.

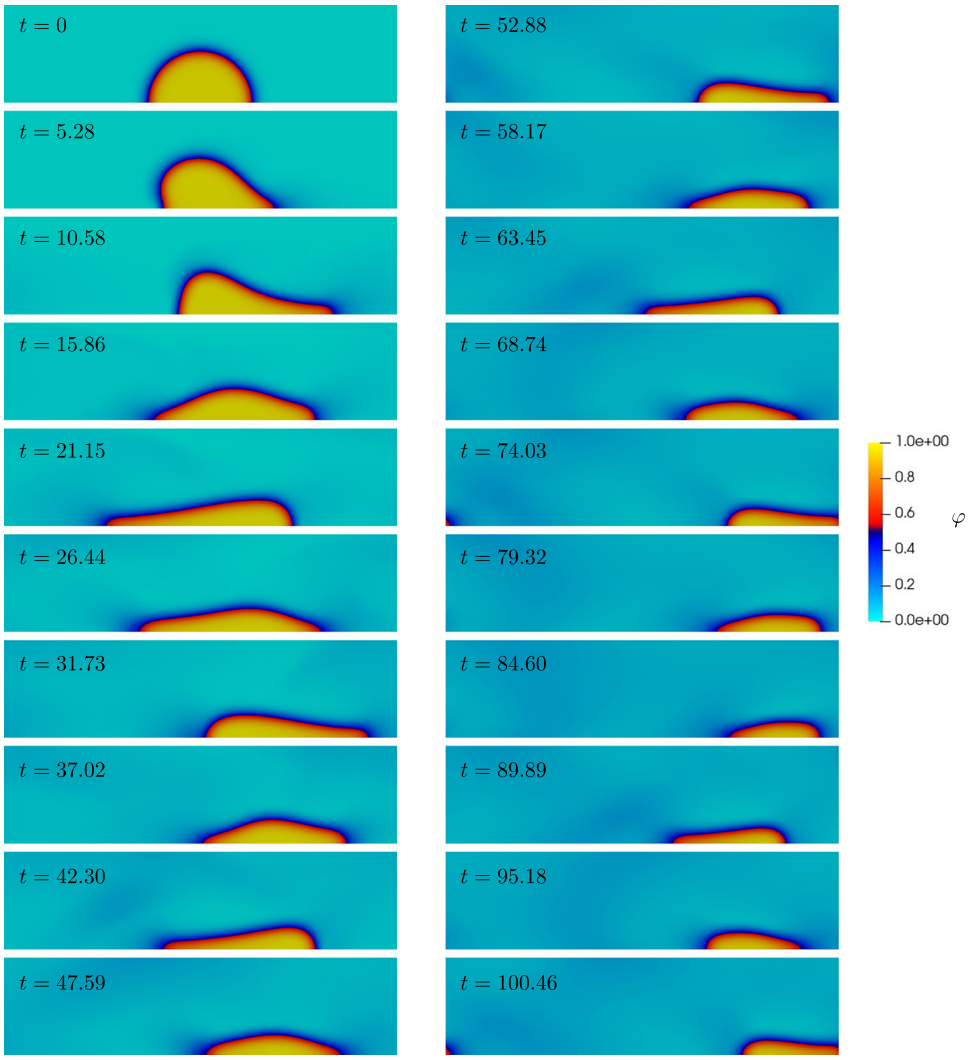

FIGURE 3 Snapshots of the simulation of a droplet with a static contact angle of 90° on a vibrating wall with $A = 10$ and $\omega = 0.3$.

stability of the obtained solution state, details of the approach can be found in [11]. The corresponding eigenshapes to the first five eigenvalues are depicted in Figure 1. The figure shows the solution state φ (Figure 1A) and the eigenshape $\varphi + ku_i$ (Figure 1B–F) where u_i is the eigenvector and k is a scaling factor to increase visibility. In all subfigures, a white contour indicating an order parameter of $\varphi = 0.5$ in the static solution is shown to highlight the approximate location of the gas-liquid interface in the solution state. A qualitative comparison of the obtained eigenshapes with known shapes of oscillating droplets, as published by Shin et al. [12] , shows good agreement.

6 | NUMERICAL EXAMPLE FOR AN OSCILLATING DROPLET

The dynamic model given by Equation (6)–(11) is used in simulations of vibrating droplets. Like the static example in section 5, the dynamic simulations were carried out in a two-dimensional domain. The vibration is achieved via an oscillation of the solid walls on the top and the bottom of the calculation domain. For this purpose, the Dirichlet boundary condition $\vec{v} = [A\omega \sin(\omega t), 0]^T$ is prescribed on the solid walls. For φ, the Neumann condition given by Equation (13) is imposed, such that the surface tensions between the fluid phases and the solid phase are taken into account. All simulations are carried out with the same values for the surface tensions as the static simulation in section 5 such that the results can be compared in a meaningful way ($\gamma_{\mathrm{lg}} = 0.581$ and $\gamma_{\mathrm{sl}} = \gamma_{\mathrm{sg}} = 0.1$). For the viscosity function in Equation (12), $a = \ln(1.09)$ and $b = -0.99$ are chosen. On the left and right boundary, periodic boundary conditions are used.

Figure 2 shows snapshots of the simulation with a wall vibration of amplitude $A = 10$ and frequency $\omega = 0.1$. The black and white contours show eigenshapes of the static solution from section 5. The contours correspond to the eigenshapes in Figure 1C and 1E. The eigenshapes are in good agreement with the results from the dynamic simulation. The analysis of the static system thus yields information about the dynamic droplet behaviour.

For the simulation results shown in Figure 3, a higher vibration frequency of $\omega = 0.3$ is chosen as a boundary condition while the other parameters remain unchanged. It is visible in Figure 3 that the droplet shrinks over time. As the mass in the whole calculation domain is conserved, the shrinkage leads to an oversaturated gas phase which is manifested by a darker coloured gas domain in Figure 3. This is due to the high vibration frequency generating a high kinetic energy which dissipates and contributes to the evaporation process.

7 | CONCLUSION

In this work, dynamic simulations of droplets on a horizontally vibrating solid wall as well as static simulations of a droplet on a fixed solid wall are carried out. This is done by combining the free energy density of a gas-liquid phase field with the Navier-Stokes equations via the Korteweg stress tensor. It is found that the eigenvalue analysis of the static system yields the possible modes of an oscillating droplet, some of which are recovered by the results of the dynamic simulations. For a high vibration frequency, it is observed that the increased kinetic energy leads to an evaporation process of the liquid droplet.

Further research is needed to systematically analyse the influence of the input parameters, such as the amplitude and the frequency of the wall vibration as well as the surface tensions, the interface width and the viscosity of the fluid, on the resulting droplet behaviour. This should also reveal if the other eigenshapes from the static simulations can be recovered. Furthermore, it might be interesting to study vibrating droplets on non-smooth surfaces to achieve a transition between wetting states, as it was shown experimentally in [13].

ACKNOWLEDGMENTS

This research was funded by the Deutsche Forschungsgemeinschaft (DFG, German Research Foundation) – Projektnummer 172116086 – SFB 926.

Open access funding enabled and organized by Projekt DEAL.

ORCID

Jana Kunz https://orcid.org/0000-0002-6683-1961

REFERENCES

1. Gomez, H., & van der Zee, K. G. (2017). Computational phase-field modeling. In E. Stein, R. Borst and T.J.R. Hughes (Eds.), *Encyclopedia of computational mechanics* (2nd ed.). John Wiley & Sons, Ltd.
2. Diewald, F., Heier, M., Lautenschläger, M., Lautenschläger, M., Horsch, M., Kuhn, C., Langenbach, K., Hasse, H., & Müller, R. (2019). A navier-stokes-Korteweg model for dynamic wetting based on the pets equation of state. *Proceedings in Applied Mathematics and Mechanics*, *19*, e201900091.
3. Amon, C. H., Murthy, J., Yao, S., Narumanchi, S., Wu, C. F., & Hsieh, C. C. (2001). MEMS-enabled thermal management of high-heat-flux devices EDIFICE: Embedded droplet impingement for integrated cooling of electronics. *Experimental Thermal and Fluid Science*, *25*(5), 231–242.
4. Diewald, F., Kuhn, C., Heier, M., Horsch, M., Langenbach, K., Hasse, H., & Müller, R. (2017). Surface wetting with droplets: A phase field approach. *Proceedings in Applied Mathematics and Mechanics*, *17*(1), 501–502.
5. Diewald, F., Heier, M., Horsch, M., Kuhn, C., Langenbach, K., Hasse, H., & Müller, R. (2018). Three-dimensional phase field modeling of inhomogeneous gas-liquid systems using the PeTS equation of state. *The Journal of Chemical Physics*, *149*(6), 064701.
6. Diewald, F., Lautenschlaeger, M. P., Stephan, S., Langenbach, K., Kuhn, C., Seckler, S., Bungartz, H. J., Hasse, H., & Müller, R. (2020). Molecular dynamics and phase field simulations of droplets on surfaces with wettability gradient. *Computer Methods in Applied Mechanics and Engineering*, *361*, 112773.
7. Diewald, F., Heier, M., Lautenschläger, M., Kuhn, C., Langenbach, K., Hasse, H., & Müller, R. (2021). Phase field simulations of wetting based on molecular simulations. *Proceedings in Applied Mathematics and Mechanics*, *20*, e202000035.
8. Moelans, N., Blanpain, B., & Wollants, P. (2008). An introduction to phase-field modeling of microstructure evolution. *Calphad*, *32*(2), 268–294.
9. Anderson, D. M., McFadden, G. B., & Wheeler, A. A. (1998). DIFFUSE-INTERFACE METHODS IN FLUID MECHANICS. *Annual Review of Fluid Mechanics*, *30*(1), 139–165.

10. Diewald, F. (2020). *Phase Field Modeling of Static and Dynamic Wetting* (Doctoral thesis). Technische Universität Kaiserslautern.
11. Diewald, F., Kuhn, C., Heier, M., Langenbach, K., Horsch, M., Hasse, H., & Müller, R. (2018). Investigating the stability of the phase field solution of equilibrium droplet configurations by eigenvalues and eigenvectors. *Computational Materials Science*, *141*, 185–192.
12. Shin, Y. S., & Lim, H. C. (2014). Shape oscillation and detachment conditions for a droplet on a vibrating flat surface. *The European Physical Journal E*, *37*(8), 30.
13. Lei, W., Jia, Z. H., He, J. C., Cai, T. M., & Wang, G. (2014). Vibration-induced wenzel-cassie wetting transition on microstructured hydrophobic surfaces. *Applied Physics Letters*, *104*(18), 181601.

How to cite this article: Kunz, J., Rutz, X., Stephan, S., Hasse, H., & Müller, R. (2023). Simulation of vibrating droplets using a phase field approach. *Proceedings in Applied Mathematics and Mechanics*, *23,* e202300232. https://doi.org/10.1002/pamm.202300232